

The Dam1 kinetochore ring complex moves processively on depolymerizing microtubule ends

Stefan Westermann¹, Hong-Wei Wang², Agustin Avila-Sakar², David G. Drubin¹, Eva Nogales^{1,2,3} & Georjana Barnes¹

Chromosomes interact through their kinetochores with microtubule plus ends and they are segregated to the spindle poles as the kinetochore microtubules shorten during anaphase A of mitosis. The molecular natures and identities of coupling proteins that allow microtubule depolymerization to pull chromosomes to poles during anaphase have long remained elusive¹. In budding yeast, the ten-protein Dam1 complex is a critical microtubule-binding component of the kinetochore² that oligomerizes into a 50-nm ring around a microtubule *in vitro*^{3,4}. Here we show, with the use of a real-time, two-colour fluorescence microscopy assay, that the ring complex moves processively for several micrometres at the ends of depolymerizing microtubules without detaching from the lattice. Electron microscopic analysis of 'end-on views' revealed a 16-fold symmetry of the kinetochore rings. This out-of-register arrangement with respect to the 13-fold microtubule symmetry is consistent with a sliding mechanism based on an electrostatically coupled ring-microtubule interface. The Dam1 ring complex is a molecular device that can translate the force generated by microtubule depolymerization into movement along the lattice to facilitate chromosome segregation.

Although in principle minus-end-directed motor proteins could be responsible for the poleward transport of chromosomes, it has long been recognized that the force generated by microtubule depolymerization itself contributes to movements during anaphase A^{1,5}. Microtubule depolymerization is sufficient to move metazoan chromosomes⁶ or kinesin-coated microbeads *in vitro*^{7,8}. Different theoretical models have tried to explain how kinetochores exploit the force created by depolymerization^{9,10}, but the molecular nature of a device that would remain attached to a disassembling microtubule end without losing its connection has remained elusive.

Budding yeast mitosis displays anaphase A and B movements¹¹, and kinetochore microtubule dynamics are restricted to plus ends¹². Recent studies have revealed that the budding yeast kinetochore is composed of at least eight multiprotein complexes that assemble on centromeric DNA in a hierarchical manner^{13–15}. A critical microtubule binding activity of the kinetochore is provided by the ten-protein Dam1 complex, which is essential for mitotic spindle integrity and, under regulation by the yeast Aurora B kinase Ipl1p, for the establishment and maintenance of bipolar chromosome attachments^{16–18}.

Purified Dam1 complex oligomerizes into 50-nm ring structures when incubated with microtubules *in vitro*^{3,4}. The Dam1 rings form at physiologically relevant concentrations, encircle the microtubule orthogonal to its axis, promote microtubule assembly, and preferentially bind to the GTP lattice of GTP/GDP-segmented microtubules, suggesting a mechanism for their targeting to plus ends³. Two observations suggested that the ring complex might exhibit lateral

mobility on the microtubule: first, the nature of the interaction between rings and microtubules is largely electrostatic, and second, electron micrographs of the Dam1 ring complex showed that rings accumulated at the ends of depolymerizing microtubules³.

To uncover the principles of force generation and motility at the kinetochore we sought to develop a fluorescence microscopy assay that would allow observation of the Dam1 complex on dynamic microtubules in real time. The main challenge was to observe microtubules that are not completely attached to the surface of a flow cell because this might impede movement of the ring complex. This was achieved by imaging the microtubules in a flow chamber filled with a viscous solution of methylcellulose and by blocking the glass surfaces to limit non-specific adsorption¹⁹ (Fig. 1a). To mimic microtubule dynamics during anaphase we induced depolymerization either by including the kinesin13 family member XMCAK1 in the motility buffer or by diluting Dam1-decorated microtubules below the critical concentration for microtubule assembly. Indistinguishable results were obtained by both disassembly protocols. When 5 nM Alexa488-conjugated Dam1 complex was incubated with rhodamine-labelled microtubules, which were then diluted, microtubules depolymerized over the course of several minutes. As the free end of the microtubule shortened, the Alexa488 signal could clearly be seen tracking with the disassembling end (Fig. 1b and Supplementary Movie S1). In cases where the observed microtubule was completely free in solution, Dam1 signals tracked both depolymerizing ends and increased in intensity as the microtubule shortened (Supplementary Movie S2). In rare events, the Dam1 signal was partly released from the depolymerizing end, probably as a result of adsorption of the complex to the coverslip surface. In these cases, the green fluorescent Dam1 signal was 'stretched' before release, demonstrating the force generated by the depolymerizing microtubule end (Supplementary Movie S3).

In principle, tracking could occur through one of two different mechanisms: continued association of an intact ring with the microtubule lattice ('sliding'), or the rapid dissociation and reassociation of ring subunits with the retracting microtubule end ('turn-over'). To distinguish between these possibilities, we mixed green fluorescent Alexa488–Dam1 complex with red fluorescent Alexa594–Dam1 complex and incubated this mixture with unlabelled microtubules; after incubation for 30 min we visualized them in our assay system. Because rings were formed by randomly combining green and red fluorescent complexes, each spot on the microtubule showed a strict co-localization of green and red signals (Fig. 1c). In the next experiment, we added green and then red fluorescent Dam1 complex sequentially to microtubules. If the rings turned over, one would expect the subunits to re-equilibrate such that the spots on the microtubules would be green and red as in Fig. 1c. However, in this

¹Department of Molecular and Cell Biology, ²Lawrence Berkeley National Laboratory, ³Howard Hughes Medical Institute, University of California Berkeley, Berkeley, California 94720-3202, USA.

experiment most spots on the microtubule were either red or green (Fig. 1d). The rare cases in which red and green signals seemed to colocalize probably arose from adjacent rings on the microtubule too close to be resolved by fluorescence microscopy. We conclude that under our assay conditions, once bound to the microtubule, the ring subunits do not turn over and the ring tracks with the depolymerizing microtubule end as an intact entity.

We next tested whether the ring complex can couple microtubule depolymerization to the movement of a cargo. We prepared modified Dam1 rings by combining green fluorescent complexes with biotinylated complexes. These Dam1 rings readily recruited streptavidin-

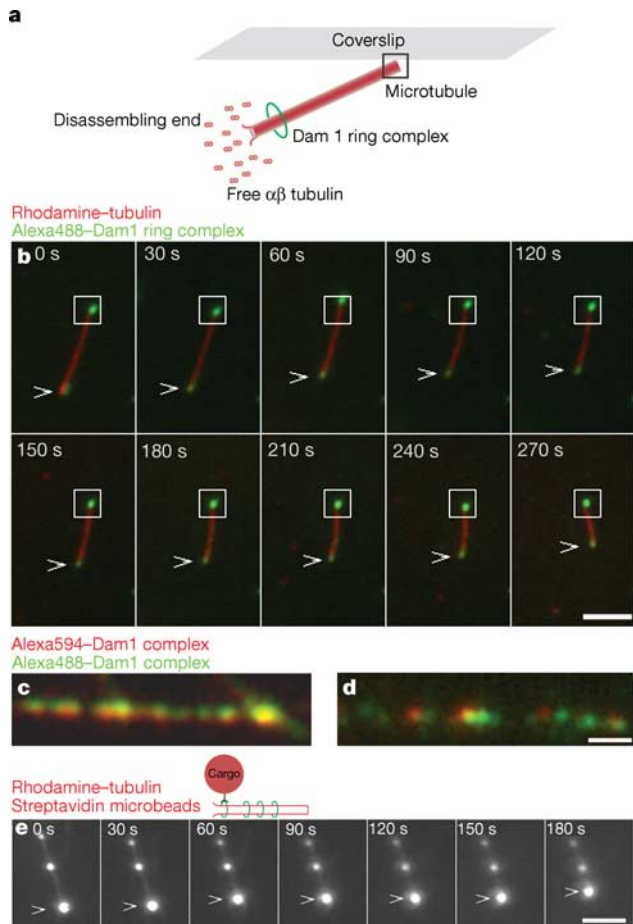


Figure 1 | A microscopy assay to study the interaction of the Dam1 complex with dynamic microtubules *in vitro*. **a**, Sketch of the assay. Observation of Dam1 ring (green) behaviour requires microtubules (red) that are attached to the coverslip with only one end or are completely free in solution. **b**, The Dam1 ring complex moves processively at the ends of depolymerizing microtubules. Time-lapse images of a microtubule (red) attached with one end to the coverslip (boxed area) while its free end depolymerizes after dilution. The Alexa488–Dam1 complex (green) follows the depolymerizing end (white arrowhead) without detaching from the lattice. Note that the fluorescent signal of the complex does not decrease significantly over the time of observation. Scale bar, 2 μm . See also Supplementary Movies S1, S2 and S3. **c**, Experiment to test for turnover of ring subunits. Green and red fluorescent Dam1 complexes are first mixed, incubated with unlabelled microtubules, and then visualized. Each spot on the microtubule shows colocalization of red and green ring segments. **d**, Green fluorescent complex is incubated with microtubules first, then red fluorescent complex is added. Spots on the microtubule corresponding to Dam1 rings are either red or green, demonstrating that there is no turnover or exchange of ring subunits. Scale bar, 1 μm . **e**, Coupling of a cargo to Dam1 rings. Time-lapse images of Dam1-coupled microbeads on depolymerizing microtubule ends (see also Supplementary Movie S4). Depolymerization was induced by adding XMCAK1. Scale bar, 5 μm .

coated, red fluorescent microbeads to microtubules (Supplementary Fig. 1). After the induction of depolymerization, the beads remained attached to Dam1-decorated depolymerizing microtubule ends and were translocated in the direction of depolymerization (Fig. 1e and Supplementary Movie S4). This result shows that the ring complex can act as a coupling device under load to move objects with the depolymerizing microtubule end.

Next we investigated the behaviour of multiple well-spaced Dam1 ring complexes on depolymerizing microtubule ends. As the microtubule disassembled, the distal Dam1 signal tracked with the end and merged with the next signal; both continued to move together with increased fluorescence intensity (Fig. 2a and Supplementary Movie 5). This ‘collection’ of Dam1 signals is further illustrated by a kymograph representation (Fig. 2b), which shows oblique Dam1 lines that merge and increase in intensity as a function of time. We quantified the Alexa488 signal of the depolymerizing end and found that it increased in steps of approximately equal magnitude. In

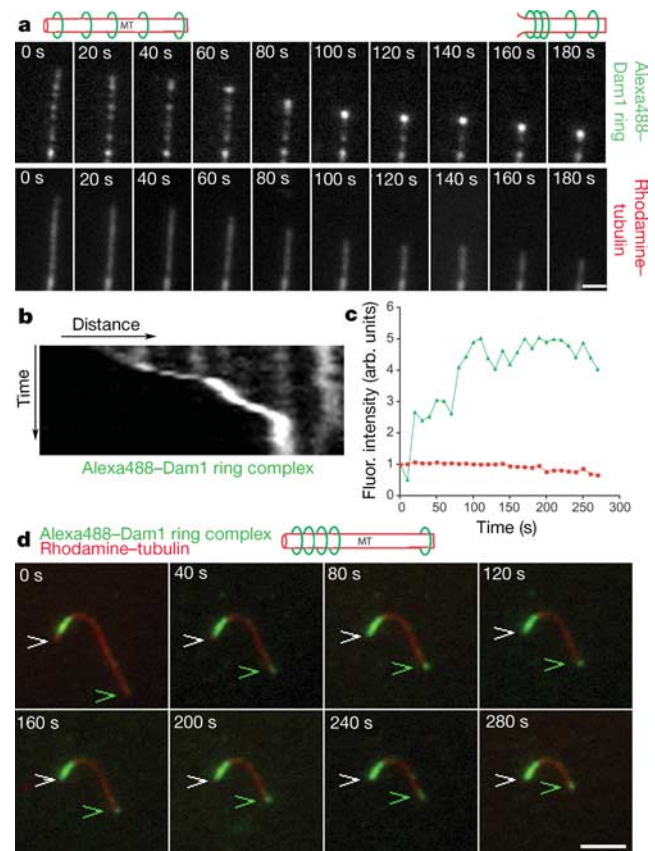


Figure 2 | Collection of multiple Dam1 rings at a depolymerizing microtubule end. **a**, Individual Dam1 rings are ‘collected’ by the depolymerizing microtubule (MT) end. Dam1 signals merge at the depolymerizing end and the fluorescence intensity increases. Depolymerization was induced by dilution. **b**, Kymograph of the Alexa488 signal from **a**, showing the behaviour of individual Dam1 rings. Note that individual lines merge, and then move together with increased intensity. **c**, Quantification of fluorescence intensity of the Alexa488 signal at the depolymerizing microtubule end. Note that the intensity does not increase linearly but in two major steps of equal size, corresponding to the merging of the strongest Dam1 signals. See also Supplementary Movie S5. **d**, Stabilization of depolymerizing microtubule ends depends on the Dam1 ring concentration: time-lapse images of a depolymerizing microtubule with asymmetric Dam1 decoration. Depolymerization of one end (white arrowhead) is stalled by a high concentration of Dam1 rings. The sparsely decorated end (green arrowhead) continues to depolymerize and the Dam1 ring follows the end without detaching. Depolymerization was induced by dilution. Scale bar, 2 μm . See also Supplementary Movie S6.

contrast, the intensity of the tubulin signal of the depolymerizing end remained constant over time (Fig. 2c). In many cases the collection of multiple Dam1 signals seemed to slow down or eventually stall depolymerization (Fig. 2b). For a better evaluation of the effect of Dam1 ring concentration on depolymerization rates we observed microtubules with asymmetrically distributed Dam1 rings: as shown in Fig. 2d (Supplementary Movie S6), a sparsely decorated end (green arrowhead) depolymerized over time and the Dam1 signal tracked with the end as observed previously. In contrast, the other end (white arrowhead) initially started to depolymerize (0–60 s) but then stalled at an area with a high Dam1 concentration (60–280 s). Thus, direct observation indicates that two fundamental biochemical activities of the complex, namely stabilization and mobility along the lattice, depend on the relative concentration of Dam1 rings at the microtubule ends.

We next investigated the dynamics of individual Dam1 rings on stable microtubules. Alexa488–Dam1 complex was incubated at a final concentration of 1–5 nM with Taxol-stabilized microtubules and followed by using fluorescence microscopy at high time resolution to detect small movements. On observation of the whole field, numerous Dam1 spots could be seen undergoing small random motions without directional preference (Supplementary Movie S7). On single Taxol-stabilized microtubules individual Dam1 spots moved independently of each other, changed direction, merged, and separated again (Fig. 3a and Supplementary Movie S8). In contrast, Dam1 signals that were adsorbed on the coverslip surface

remained immobile (Supplementary Movie S9). Thus, individual Dam1 rings show undirected, one-dimensional diffusion on a stable microtubule lattice. The mean-square displacement of individual spots increased linearly as a function of time (Fig. 3b). From the slope of the graph we calculated an average diffusion constant of about $0.54 \times 10^{-9} \text{ cm}^2 \text{ s}^{-1}$ for the movement, which is comparable to values reported for other microtubule–motor–protein systems^{7,20}.

The sliding of a ring complex along the lattice is a previously unobserved mode of microtubule-based motility and we sought to investigate structural determinants for such a mechanism. When we saturated Taxol-stabilized microtubules with Dam1 complex and revealed the sample by negative-stain electron microscopy, we occasionally observed ‘end-on views’ that provided axial projections of the microtubule–Dam1 complex arrangement (Fig. 4a). In the best three images the number of protofilaments (13) could clearly be counted, but the individual Dam1 complexes in the ring density around the microtubule were not as well defined. We performed rotational analysis on three end-on images after masking out the

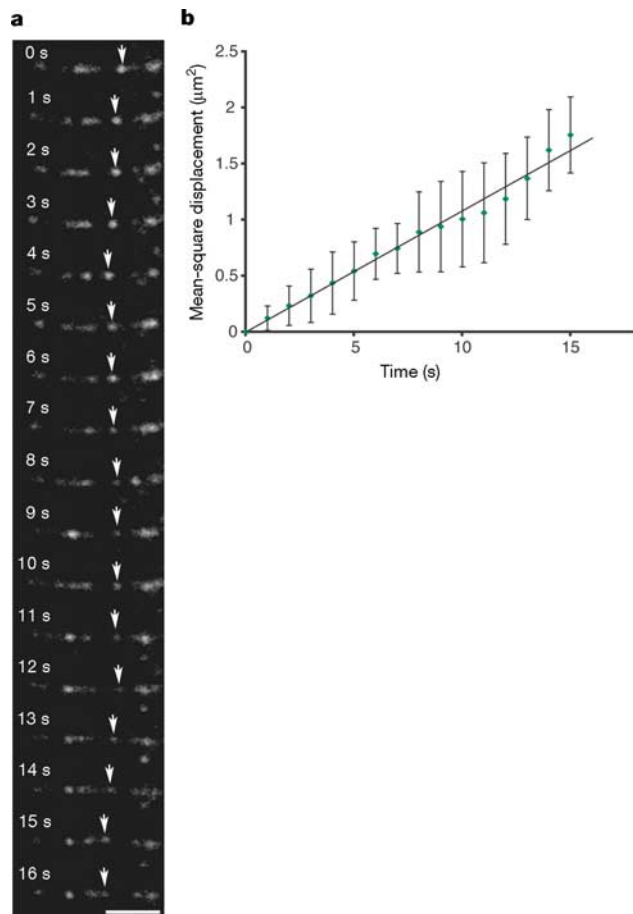


Figure 3 | One-dimensional diffusion of Dam1 rings on stable microtubules. **a**, An individual Dam1 spot on a Taxol-stabilized microtubule is followed over time. Note that it moves in both directions while other spots merge and separate again. Scale bar, 2 μm . **b**, Plot of mean-square displacement of individual Dam1 signals against time. Error bars show standard deviation. See also Supplementary Movies S7, S8 and S9.

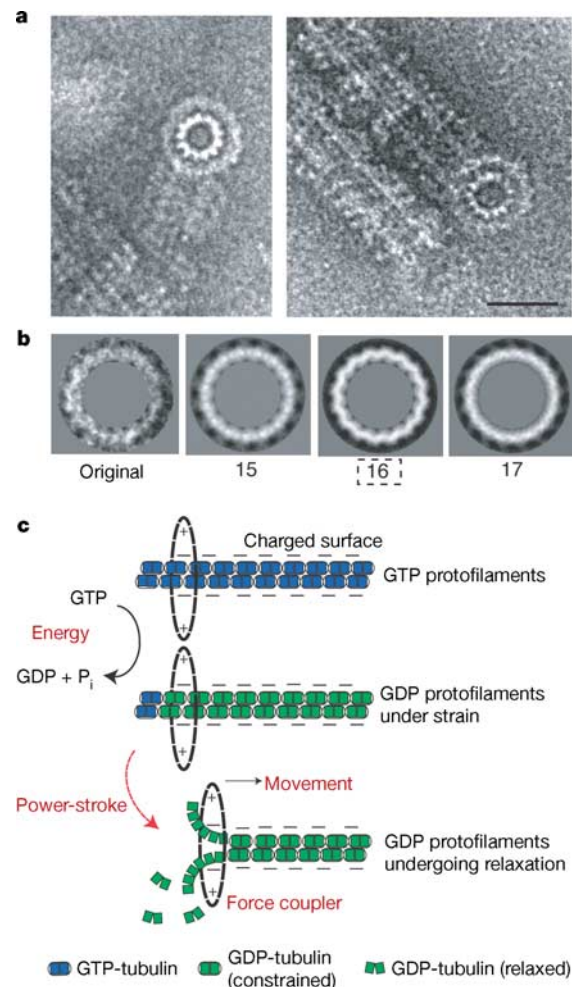


Figure 4 | Image analysis of the Dam1 ring complex around microtubules. **a**, Examples of electron micrographs showing ‘end-on views’ of microtubules surrounded with Dam1 complex. Scale bar, 50 nm. **b**, Rotational averaging of Dam1 complexes in ‘end-on views’. Original ring complex and reconstructions assuming different rotational symmetries are shown. A reconstruction with a 16-fold rotational symmetry shows sharper features and most closely resembles the original complexes. **c**, Model for Dam1 ring dynamics and function at the depolymerizing microtubule end. The free energy of GTP hydrolysis is released as peeling protofilaments produce a power-stroke by means of a transition from straight to curved. The Dam1 complex transduces this mechanical energy into directed sliding along the microtubule lattice to pull chromosomes apart during anaphase.

microtubule density. This analysis revealed a consistent 16-fold symmetry for the Dam1 ring. The sharpness of different rotational averages of the ring density at and around the correct rotational symmetry supports the cross-correlation analysis and provides a signal-enhanced view of the arrangement of the 16 Dam1 complexes as they form a ring around the microtubule (Fig. 4b).

The symmetry mismatch between the 13-fold microtubule and the 16-fold Dam1 ring suggests that there might not be specific interactions between the surface of the microtubule and the Dam1 ring. Other combinations of microtubules (14 protofilament microtubules assembled with guanosine-5'-[(α,β)-methylene]triphosphate (GMPCPP)) and Dam1 rings (18-fold for instance) were also observed with symmetry mismatch. These observations, and the requirement of the tubulin C termini for the interaction with and assembly of the Dam1 rings, are consistent with a sliding mechanism in which positive charges in the inner surface of the Dam1 ring interact electrostatically with the negative charges along the microtubule surface³.

Thus, we have obtained conclusive evidence that the Dam1 ring complex, a critical microtubule-binding element of the budding yeast kinetochore, diffuses along the microtubule lattice and moves processively with the end of a depolymerizing microtubule. This processive movement could help chromosomes to stay attached to disassembling kinetochore microtubules during anaphase A and contribute to the successful segregation of chromosomes in the absence of minus-end-directed motors. Typically, microtubules have been viewed as static tracks along which motor proteins transport cargo. However, microtubules themselves produce pushing and pulling forces that can move cellular structures²¹. Our analysis of Dam1 motility shows that the microtubule end and the ring complex form a molecular machine that generates movement (Fig. 4c). Because the GTP and GDP forms of microtubule protofilaments differ in their preferred conformations^{22,23}, the chemical energy of GTP hydrolysis is stored as mechanical strain in the lattice and is released as a power-stroke by the outward peeling of protofilaments^{24–26}. The ring is needed as a force-coupling device that translates the mechanical energy of the power-stroke into a sustained movement along the lattice. As the ring moves in response to the polymerization state of the microtubule end, we also note that it could be part of the tension-sensing machinery that monitors kinetochore–microtubule attachments²⁷.

Despite its remarkable properties *in vitro*, the Dam1 complex is clearly not the only factor that contributes to dynamic kinetochore attachment at microtubule ends *in vivo*. Some chromosome segregation occurs in *dam1* mutants at the restrictive temperature, and the fission yeast Dam1 complex, although also contributing to high-fidelity chromosome segregation, is not essential for viability^{28,29}. The Dam1 complex could be especially important in budding yeast because only one microtubule attaches to each kinetochore.

METHODS

***In vitro* assays.** Alexa488-labelled or 594-labelled Dam1 complex was prepared as described, and electron microscopy showed regular ring formation of the complex³. In an analogous procedure, biotin-maleimide (Sigma) was coupled to Dam1 complex and free biotin was separated by gel filtration. Flow cells were constructed with two layers of double-sided tape and 12 mm \times 12 mm coverslips to create a chamber volume of about 15 μ l. To block surfaces they were pretreated with 0.2% (w/v) Pluronic F108 (BASF) in PEM medium (80 mM PIPES/KOH pH 6.8, 1 mM MgCl₂, 1 mM EGTA). Motility reactions (20 μ l) contained 0.8% (w/v) methylcellulose (Sigma), 0.2% (w/v) Pluronic F108, 200 μ g ml⁻¹ glucose oxidase, 35 μ g ml⁻¹ catalase, 4.5 mg ml⁻¹ glucose, 0.5% 2-mercaptoethanol, 1 mg ml⁻¹ BSA and 0.5 mg ml⁻¹ casein in PEM and the indicated amounts of Alexa488–Dam1 complex and microtubules. To follow XMcAK1-catalysed depolymerization, 1 μ l of rhodamine-labelled GMPCPP microtubules (15 μ M) was incubated with 1 μ l of Alexa488–Dam1 complex (0.4 μ M) for 5 min at 37 °C. Then 1 μ l of the mixture was combined with 19 μ l of motility buffer containing 15 nM XMcAK1 and 1.5 mM MgATP. Alternatively, 30 μ M microtubules were assembled in the presence of 1 mM GTP and 25% (v/v) glycerol, and 1 μ l of these microtubules was then incubated with 1 μ l of Alexa488–Dam1 complex and the

sample was diluted 1:10 into motility buffer containing 8 μ M unlabelled tubulin. The sample was introduced into the flow cell and observed immediately at 25 °C on an inverted Olympus IX 81 epi-illuminated microscope with a 100 \times objective (numerical aperture 1.4) and neutral-density filters. For the observation of processive movements on depolymerizing microtubule ends, two-channel movies were made with a green fluorescent protein/red fluorescent protein filter set and motorized excitation and emission filter-wheels. The camera and the filter-wheels were controlled by Metamorph software (Universal Imaging). General processing of movies and images was performed with the ImageJ software (rsb.info.nih.gov/ij/).

Electron microscopy and symmetry analysis. Microtubule–Dam1 complexes were revealed by electron microscopy of negatively stained samples. Dam1 complex (20 μ l, 30 μ M) was incubated with 20 μ l of Taxol-stabilized microtubules (3.75 μ M) for 15 min at 37 °C, pelleted at 139,000g in a TL100 rotor and resuspended in 40 μ l of PEM (containing 1 mM GTP and 10 μ M Taxol). The sample was stained with uranyl acetate and electron microscopic images were recorded as described previously³. The rotational symmetry of the Dam1 complexes around the microtubules as seen in end-on views was analysed with the SPIDER image processing package³⁰. The end-on microtubule–Dam1 ring image was translated so that its rotation centre coincided with the image centre. The microtubule density was masked so that only the outer density corresponding to the Dam1 ring remained. The ring was then rotated at different angles and the cross-correlation coefficients with the original ring were calculated. A maximum in the cross-correlation profile as a function of the rotation angle was found every 22.5°, corresponding to a 16-fold rotational symmetry. Different rotational averages of the Dam1 ring density at and around the correct rotational symmetry (16-fold) were then calculated with SPIDER.

Received 22 September; accepted 9 November 2005.

Published online 15 January 2006.

- Maiato, H., Deluca, J., Salmon, E. D. & Earnshaw, W. C. The dynamic kinetochore–microtubule interface. *J. Cell Sci.* **117**, 5461–5477 (2004).
- Cheeseman, I. M. *et al.* Implication of a novel multiprotein Dam1p complex in outer kinetochore function. *J. Cell Biol.* **155**, 1137–1145 (2001).
- Westermann, S. *et al.* Formation of a dynamic kinetochore–microtubule interface through assembly of the Dam1 ring complex. *Mol. Cell* **17**, 277–290 (2005).
- Miranda, J. J., De Wulf, P., Sorger, P. K. & Harrison, S. C. The yeast DASH complex forms closed rings on microtubules. *Nature Struct. Mol. Biol.* **12**, 138–143 (2005).
- Inoue, S. & Salmon, E. D. Force generation by microtubule assembly/disassembly in mitosis and related movements. *Mol. Biol. Cell* **6**, 1619–1640 (1995).
- Koshland, D. E., Mitchison, T. J. & Kirschner, M. W. Polewards chromosome movement driven by microtubule depolymerization *in vitro*. *Nature* **331**, 499–504 (1988).
- Lombillo, V. A., Stewart, R. J. & McIntosh, J. R. Minus-end-directed motion of kinesin-coated microspheres driven by microtubule depolymerization. *Nature* **373**, 161–164 (1995).
- Coue, M., Lombillo, V. A. & McIntosh, J. R. Microtubule depolymerization promotes particle and chromosome movement *in vitro*. *J. Cell Biol.* **112**, 1165–1175 (1991).
- Hill, T. L. Theoretical problems related to the attachment of microtubules to kinetochores. *Proc. Natl Acad. Sci. USA* **82**, 4404–4408 (1985).
- Molodtsov, M. I., Grishchuk, E. L., Efremov, A. K., McIntosh, J. R. & Ataulkhanov, F. I. Force production by depolymerizing microtubules: a theoretical study. *Proc. Natl Acad. Sci. USA* **102**, 4353–4358 (2005).
- Straight, A. F., Marshall, W. F., Sedat, J. W. & Murray, A. W. Mitosis in living budding yeast: anaphase A but no metaphase plate. *Science* **277**, 574–578 (1997).
- Maddox, P. S., Bloom, K. S. & Salmon, E. D. The polarity and dynamics of microtubule assembly in the budding yeast *Saccharomyces cerevisiae*. *Nature Cell Biol.* **2**, 36–41 (2000).
- De Wulf, P., McAinsh, A. D. & Sorger, P. K. Hierarchical assembly of the budding yeast kinetochore from multiple subcomplexes. *Genes Dev.* **17**, 2902–2921 (2003).
- Westermann, S. *et al.* Architecture of the budding yeast kinetochore reveals a conserved molecular core. *J. Cell Biol.* **163**, 215–222 (2003).
- Cheeseman, I. M., Drubin, D. G. & Barnes, G. Simple centromere, complex kinetochore: linking spindle microtubules and centromeric DNA in budding yeast. *J. Cell Biol.* **157**, 199–203 (2002).
- Cheeseman, I. M., Enquist-Newman, M., Muller-Reichert, T., Drubin, D. G. & Barnes, G. Mitotic spindle integrity and kinetochore function linked by the Duo1p/Dam1p complex. *J. Cell Biol.* **152**, 197–212 (2001).
- Cheeseman, I. M. *et al.* Phospho-regulation of kinetochore-microtubule attachments by the Aurora kinase Iplp. *Cell* **111**, 163–172 (2002).
- Tanaka, K. *et al.* Molecular mechanisms of kinetochore capture by spindle microtubules. *Nature* **434**, 987–994 (2005).

19. Kapitein, L. C. *et al.* The bipolar mitotic kinesin Eg5 moves on both microtubules that it crosslinks. *Nature* **435**, 114–118 (2005).
20. Vale, R. D., Soll, D. R. & Gibbons, I. R. One-dimensional diffusion of microtubules bound to flagellar dynein. *Cell* **59**, 915–925 (1989).
21. Howard, J. & Hyman, A. A. Dynamics and mechanics of the microtubule plus end. *Nature* **422**, 753–758 (2003).
22. Wang, H. W. & Nogales, E. Nucleotide-dependent bending flexibility of tubulin regulates microtubule assembly. *Nature* **435**, 911–915 (2005).
23. Hyman, A. A., Chretien, D., Arnal, I. & Wade, R. H. Structural changes accompanying GTP hydrolysis in microtubules: information from a slowly hydrolyzable analogue guanylyl-(α,β)-methylene-diphosphonate. *J. Cell Biol.* **128**, 117–125 (1995).
24. Mandelkow, E. M., Mandelkow, E. & Milligan, R. A. Microtubule dynamics and microtubule caps: a time-resolved cryo-electron microscopy study. *J. Cell Biol.* **114**, 977–991 (1991).
25. Mahadevan, L. & Mitchison, T. J. Cell biology: powerful curves. *Nature* **435**, 895–897 (2005).
26. Grishchuk, E. L., Molodtsov, M. I., Ataulkhanov, F. I. & McIntosh, J. R. Force production by disassembling microtubules. *Nature* **438**, 384–388 (2005).
27. Pinsky, B. A. & Biggins, S. The spindle checkpoint: tension versus attachment. *Trends Cell Biol.* **15**, 486–493 (2005).
28. Liu, X., McLeod, I., Anderson, S., Yates, J. R. & He, X. Molecular analysis of kinetochore architecture in fission yeast. *EMBO J.* **24**, 2919–2930 (2005).
29. Sanchez-Perez, I. *et al.* The DASH complex and Klp5/Klp6 kinesin coordinate bipolar chromosome attachment in fission yeast. *EMBO J.* **24**, 2931–2943 (2005).
30. Frank, J. *et al.* SPIDER and WEB: processing and visualization of images in 3D electron microscopy and related fields. *J. Struct. Biol.* **116**, 190–199 (1996).

Supplementary Information is linked to the online version of the paper at www.nature.com/nature.

Acknowledgements We thank C. Walczak for the gift of recombinant XMCAK1; M. Kaksonen and C. Toret for help with image analysis; and all members of the Barnes/Drubin laboratory for discussions. This work was supported by grants from the National Institute of General Medical Sciences to G.B. and E.N., and from the Office of Basic Energy Science of the US Department of Energy. E.N. is a Howard Hughes Medical Institute Investigator. Research in this study was in part supported by a grant to D.G.D. from Phillip Morris USA Inc. and Phillip Morris International and by a postdoctoral fellowship of the Deutsche Forschungsgemeinschaft to S.W.

Author Information Reprints and permissions information is available at npg.nature.com/reprintsandpermissions. The authors declare no competing financial interests. Correspondence and requests for materials should be addressed to G.B. (gbarnes@socrates.berkeley.edu).